ORIGINAL ARTICLE

Nontargeted Lipidomic Characterization of Porcine Organs Using Hydrophilic Interaction Liquid Chromatography and Off-Line Two-Dimensional Liquid Chromatography–Electrospray Ionization Mass Spectrometry

Eva Cífková · Michal Holčapek · Miroslav Lísa

Abstract Lipids form a significant part of animal organs and they are responsible for important biological functions, such as semi-permeability and fluidity of membranes, signaling activity, anti-inflammatory processes, etc. We have performed a comprehensive nontargeted lipidomic characterization of porcine brain, heart, kidney, liver, lung, spinal cord, spleen, and stomach using hydrophilic interaction liquid chromatography (HILIC) coupled to electrospray ionization mass spectrometry (ESI/MS) to describe the representation of individual lipid classes in these organs. Detailed information on identified lipid species inside classes are obtained based on relative abundances of deprotonated molecules $[M-H]^-$ in the negative-ion ESI mass spectra, which provides important knowledge on phosphatidylethanolamines and their different forms of fatty acyl linkage (ethers and plasmalogens), phosphatidylinositols, and hexosylceramides containing nonhydroxy- and hydroxy-fatty acyls. The detailed analysis of identified lipid classes using reversed-phase liquid chromatography in the second dimension was performed for porcine brain to determine more than 160 individual lipid species containing attached fatty acyls of different acyl chain length, double-bond number, and positions on the glycerol skeleton. The fatty acid composition of porcine organs is determined by gas chromatography with flame ionization detection after the transesterification with sodium methoxide.

Abbreviations

APCI	Atmospheric pressure chemical ionization
CE	Cholesteryl ester
Cer	Ceramide
Chol (C)	Cholesterol
CN	Carbon number
DB	Double bond
ESI	Electrospray ionization
ePC (PakCho)	Plasmanylphosphatidylcholine (ether)
ePE (PakEtn)	Plasmanylphosphatidylethanolamine (ether)
FAME	Fatty acid methyl ester
FID	Flame ionization detector
GC	Gas chromatography
HexCer	Hexosylceramide
HILIC	Hydrophilic interaction liquid chromatography
HPLC	High-performance liquid chromatography
IS	Internal standard
LPC (LysoPtdCho)	Lysophosphatidylcholine
LPE (LysoPtdEtn)	Lysophosphatidylethanolamine
MS	Mass spectrometry
NARP	Nonaqueous reversed-phase
PC (PtdCho)	Choline glycerophospholipids
PE (PtdEtn)	Ethanolamine glycerophospholipids

E. Cífková · M. Holčapek (✉) · M. Lísa
Department of Analytical Chemistry, Faculty of Chemical Technology, University of Pardubice, Studentská 573, 532 10 Pardubice, Czech Republic
e-mail: michal.holcapek@upce.cz

PI (PtdIns)	Phosphatidylinositol
PG (PtdGro)	Phosphatidylglycerol
pPC (PlsCho)	Plasmenylphosphatidylcholine (plasmalogen)
pPE (PlsEtn)	Plasmenylphosphatidylethanolamine (plasmalogen)
PS (PtdSer)	Phosphatidylserine
QqQ	Triple quadrupole
RF	Response factor
RP	Reversed-phase
SM (CerPCho)	Sphingomyelin
SRM	Selected reaction monitoring
TG (TAG)	Triacylglycerol

Introduction

Lipids are important components of cellular organisms that serve as building blocks of membranes, sources of energy, essential fatty acids and fat-soluble vitamins, biosynthetic precursor of cellular components, transmission of information in cells, etc. [1–3]. They are divided according to their structural and biosynthetic complexity into the following categories: fatty acyls, glycerolipids, glycerophospholipids, sphingolipids, sterol lipids, prenol lipids, saccharolipids, and polyketides [1]. Fatty acids are building blocks for the synthesis of triacylglycerols (TG), which are mainly used for energy storage and signaling. The balance among saturated, monounsaturated, and polyunsaturated fatty acids is important for maintaining the optimum fluidity of membranes. In the human organism, polyunsaturated fatty acids (PUFA) are main components of brain and retina, and n-6 PUFA are essential for the biosynthesis of prostaglandins, which decreases the production of inflammatory agents [4]. Glycerophospholipids are key constituents of lipid bilayers, which form the separate environment of internal cells and participate in the cellular signaling and enzyme activation. In nature, glycerophospholipids containing ether-linked fatty acyls (plasmenyl and plasmanyl-lipids) instead of ester-linked fatty acyls are common, especially as membrane constituents. Plasmenyl-lipids (plasmalogens) form up to 50 % of glycerophospholipids of brain and heart tissues of human, while plasmanyl-lipids (ethers) occur at only a few percent, but elevated levels of plasmalogens have been reported in human cancer tissues [5–7]. Sphingolipids are contained in most cell membranes, mainly in nervous membranes (brain and spinal cord).

The comprehensive lipidomic analysis of biological samples is a daunting task due to the extreme complexity of the lipidome (amphipathic character of lipids with hydrophobic acyl tails and hydrophilic head groups). Two basic strategies are used in mass spectrometry (MS)-based analysis of lipids: (1) direct infusion approaches without any separation step (shotgun method), and (2) chromatographic separation followed by MS, typically high-performance liquid chromatography (HPLC)–MS. Gas chromatography with flame ionization detection (GC/FID) or MS detection can be used for fatty acid profiling after the transesterification to fatty acid methyl esters (FAME) [8, 9]. HPLC/MS is a powerful technique in the separation of complex mixtures of glycerolipids, glycerophospholipids, sphingolipids, etc. Nonaqueous reversed-phase (NARP) HPLC coupled to atmospheric pressure chemical ionization (APCI) MS is applicable for the separation and identification of nonpolar lipids, such as TGs [9–12]. Hydrophilic interaction liquid chromatography (HILIC) and reversed-phase (RP) HPLC coupled to electrospray ionization (ESI) MS has been used for the separation of glycerophospholipids and sphingolipids [13–18] in animal tissues. Furthermore, the coupling of thin-layer chromatography (TLC) and matrix-assisted laser desorption-ionization (MALDI) has also been applied for the analysis of biological samples [19–21]. Comprehensive lipidomic analysis is often performed using on-line or off-line two-dimensional HPLC, which offers the opportunity to separate complex lipidomic mixtures according to two molecular properties [18, 22, 23]. Another possibility for the characterization of lipid classes with different ionization behavior is dual parallel coupling of HPLC and MS, where a certain portion of effluent can be diverted into the second HPLC/MS with different chromatographic and ionization conditions than the first HPLC/MS configuration [24].

The lipidomic quantitation has been a challenge for long time, but several approaches for targeted and nontargeted quantitation of lipids are known using MS (direct infusion [25–27] or in HPLC/MS configuration [28]) or ^{31}P nuclear magnetic resonance (NMR) spectrometry [29, 30]. The most widespread shotgun approach applies the direct infusion ESI–MS using various scans typical for triple quadrupole (QqQ) [13, 14, 17, 31–35] or hydride quadrupole–linear ion trap mass analyzers [36], such as the precursor ion scan, the neutral loss scan, the product ion scan, and the selected reaction monitoring (SRM), together with the use of suitable internal standards (typically deuterated or odd carbon number analogs of determined lipids). The shotgun approach has been used in numerous lipidomic studies due to its simplicity, easy automation, and rapidity. The shotgun approach without HPLC separation is less convenient for the analysis of isobaric lipids [28]. Ion suppression/enhancement effects in the shotgun approach can be stronger compared to HPLC/MS [28]. The novel trend in the lipidomic quantitation is the use of high-resolution quadrupole–time-of-flight (Q-TOF) mass analyzer [36] or even an ultrahigh-resolution orbitrap analyzer with the Fourier transformation providing the resolving power

over 100,000 (FWHM) and sub-ppm mass accuracy [17]. HPLC/MS methods offer the separation of isobaric species and significantly reduce suppression effects, but on the other hand it takes longer and requires additional instrumentation and expertise. Typically, reversed-phase (RP) mode is used for the HPLC separation with possible identification of several hundred lipid species [17, 23]. Recently, we have introduced the nontargeted approach based on HILIC-HPLC separation of lipid classes and the determination based on the use of response factors (RFs) for individual lipid classes together with a single internal standard (sphingosyl PE, d17:1/12:0) [37]. Another nontargeted method for the lipid class quantitation is ^{31}P NMR [29, 30], which is an accurate and nondestructive method, but suffering from low sensitivity and therefore very long measurement times, and is not suitable for HPLC coupling.

The main goal of this work is the application of nontargeted a HILIC-HPLC/ESI–MS method for qualitative and quantitative characterization of the lipidome, mainly glycerophospholipids and sphingolipids, in biological tissues (porcine organs), with comparison of the results with previously published data [13, 14, 17, 30, 38–41]. In this work, we determine the distribution of individual lipid classes in porcine brain, heart, kidney, liver, lung, spinal cord, spleen, and stomach, together with the representation of fatty acyls within certain classes.

Materials and Methods

Chemicals and Standards

Acetonitrile, 2-propanol, and methanol (all HPLC gradient grade), hexane and chloroform stabilized by 0.5–1 % ethanol (both HPLC grade), sodium methoxide, and ammonium acetate were purchased from Sigma-Aldrich (St. Louis, MO, USA). 1,2-dimyristoyl-sn-glycero-3-phosphoglycerol (14:0/14:0-PG), 1,2-dimyristoyl-sn-glycero-3-phosphoethanolamine (14:0/14:0-PE), 1-myristoyl-2-hydroxy-sn-glycero-3-phosphoethanolamine (14:0-LPE), 1,2-dimyristoyl-sn-glycero-3-phosphocholine (14:0/14:0-PC), and 1-myristoyl-2-hydroxy-sn-glycero-3-phosphocholine (14:0-LPC) for the determination of extraction yields, 1,2-dipalmitoyl-sn-glycero-3-phosphocholine (16:0/16:0-PC), 1,2-dioleoyl-sn-glycero-3-phosphocholine (18:1/18:1-PC), 1,2-distearoyl-sn-glycero-3-phosphocholine (18:0/18:0-PC), 1,2-diarachidonoyl-sn-glycero-3-phosphocholine (20:4/20:4-PC), 1,2-didocosahexaenoyl-sn-glycero-3-phosphocholine (22:6/22:6-PC), 1,2-diheptadecanoyl-sn-glycero-3-phosphoethanolamine (17:0/17:0-PE), and 1,2-dioleoyl-sn-glycero-3-phosphoethanolamine (18:1/18:1-PE) for determination of ionization efficiency, and N-dodecanoyl-heptadecasphing-4-enine-1-phosphoethanolamine

(sphingosyl PE, d17:1/12:0) used as the IS for the nontargeted quantitation with RFs were purchased from Avanti Polar Lipids (Alabaster, AL, USA). Brain, heart, kidney, liver, lung, spinal cord, spleen, and stomach of pig (female at the age of 8 months) were obtained from the family farm of the first author.

Sample Preparation

Total lipid extracts for HILIC-HPLC/MS analyses were prepared according to the modified Folch procedure [42] using a chloroform–methanol–water system. Briefly, approximately 0.5 g of porcine organ and 50 μL of 3.3 mg/mL IS (sphingosyl PE, d17:1/12:0) were homogenized with 10 mL of chloroform–methanol (2:1, v/v) mixture for 5 min and the homogenate was filtered using a coarse filter paper. Then, 2 mL of 1 mol/L NaCl was added, and the mixture was centrifuged at 2,500 rpm for 4 min at ambient temperature. The chloroform (bottom) layer containing lipids was taken and evaporated by a gentle stream of nitrogen and redissolved in chloroform–2-propanol (1:1,v/v) mixture for subsequent HILIC analyses.

FAMEs for GC/FID analyses were prepared from total lipid extracts of porcine organs using a standard procedure with sodium methoxide [8]. Briefly, the amount of 200 μL of total lipid extract and 1.6 mL of 0.25 mol/L sodium methoxide in methanol was heated on a water bath for 10 min at 65 °C. After the reaction, 1 mL of water saturated with sodium chloride and 1 mL of hexane were added, and the mixture was centrifuged at 2,500 rpm for 3 min at ambient temperature. The hexane (upper) layer containing FAMEs was taken and used for GC/FID analyses.

HILIC-HPLC/ESI–MS of Individual Porcine Organs

Total lipid extracts of porcine organs were analyzed using a Spherisorb Si column (250 × 4.6 mm, 5 μm; Waters, Milford, MA, USA), a flow rate of 1 mL/min, an injection volume of 10 μL, column temperature of 40 °C and a mobile phase gradient: 0 min—94 % A + 6 % B, 60 min—77 % A + 23 % B, where A is acetonitrile and B is 5 mM aqueous ammonium acetate [18]. All HPLC/MS experiments were performed on the liquid chromatograph Agilent 1200 series (Agilent Technologies, Waldbronn, Germany) coupled to the Esquire 3000 ion trap analyzer with ESI (Bruker Daltonics, Bremen, Germany). Individual lipid classes were identified and quantified using the total ion current in positive-ion and negative-ion modes in the mass range m/z 50–1,000 with the following setting of tuning parameters: pressure of the nebulizing gas 60 psi, drying gas flow rate 10 L/min, and temperature of the drying gas 365 °C. Low-energy collision-induced

dissociation tandem mass spectrometry (MS/MS) experiments were performed during HPLC/MS runs with the automatic precursor selection, the isolation width of $\Delta m/z$ 4, the collision amplitude of 1 V, and helium as a collision gas. Data were acquired and evaluated using the Data Analysis software (Bruker Daltonics).

Off-Line 2D-HPLC/MS of Porcine Brain

Individual lipid classes from porcine brain were manually collected during the HILIC-HPLC analysis, fractions were evaporated by a gentle stream of nitrogen and redissolved in acetonitrile–2-propanol (1:1, v/v) mixture. The volume for the redissolvation was selected according to the concentration of individual fractions. In the second dimension, fractions of polar lipid classes were analyzed using RP-HPLC/MS with core–shell particles column Kinetex C_{18} (150 × 2.1 mm, 2.6 μm; Phenomenex, Torrance, CA, USA), flow rate of 0.3 mL/min, injection volume of 1 μL, separation temperature of 40 °C, and mobile phase gradient: 0 min—75 % A + 25 % B, 110 min—89 % A + 11 % B, where A is the mixture of acetonitrile–2-propanol (1:1, v/v) and B is 5 mM aqueous ammonium acetate. Polar lipids were identified using ESI–MS in the mass range m/z 50–1,500 with the following setting of tuning parameters: pressure of the nebulizing gas of 40 psi, drying gas flow rate of 9 L/min, and temperature of the drying gas 365 °C. The identification of individual lipids is done by their ESI mass spectra and the knowledge of their retention behavior in HILIC and RP modes [18, 37].

GC/FID Analyses of FAMEs

The gas chromatograph with flame ionization detection Agilent 7890 (Agilent Technologies) using TR-FAME column (70 % cyanopropyl polysilphenylene-siloxane), 60 m length, 0.25 mm ID, 0.25 μm film thickness (Thermo Scientific, Waltham, MA, USA), was used for the fatty acid profiling based on measurements of their corresponding FAMEs. GC conditions were as follows: injection volume 1 μL, split ratio 1:15, flow rate of helium as a carrier gas 1.025 mL/min, and temperature program: initial temperature 160 °C, ramp to 210 °C at 2 °C/min, and then ramp to 235 °C at 22 °C/min. Injector and detector temperatures were 250 and 280 °C, respectively.

Results and Discussion

Our nontargeted quantitation approach [37] is based on the measurement of response factors for individual lipid classes using representatives of all determined classes (i.e., lipid species containing oleic acids). This way, relative differences (i.e., response factors) for individual lipid classes are determined. The determination of basic analytical parameters of developed method has to been done before measurements of real samples, such as limit-of-quantitation (LOQ) determined at signal-to-noise ratio of 10 (10–100 nmol/g for all classes except for PI and LPE; Table S-1) and standard deviations determined from 10 replicates (below 5.5 % in all cases; Table S-1). Another issue for the reliable lipidomic quantitation is the knowledge of effects of fatty acyl chain length and the number of double bonds on the ionization efficiency, which is determined for both polarity modes (positive and negative) and both chromatographic systems (HILIC and RP) under identical conditions as used for the analysis of real samples (Table S-2). Measurements of 5 PC standards (16:0/16:0, 18:1/18:1, 18:0/18:0, 20:4/20:4, and 22:6/22:6) and 3 PE (14:0/14:0, 17:0/17:0, and 18:1/18:1) show that the relative differences in responses (related to 18:1 containing species set as 100 % response) are in the range 70–110 % for RP in both polarity modes and 77–130 % for HILIC in both polarity modes. It should be mentioned that the negative-ion mode is not convenient for the detection of choline-containing PLs due to the low sensitivity, but relative responses still fit into the above-mentioned intervals.

The rather important issue of our nontargeted quantitation of lipid classes is the verification that ratios of extraction yields among lipid classes for different samples are comparable. In addition to the determination of extraction yields reported in our previous work [37], we have performed the following spiking experiment for one lipid species per class not occurring in studied samples (Fig. S-1). The mixture of representative standards of selected lipid classes (PG, PE, LPE, PC, and LPC) containing C14:0 fatty acids (concentration 88 μg/mL of each standard) and sphingosyl PE (d17:1/12:0) as the IS (concentration 222 μg/mL) was prepared and measured by HILIC-HPLC/ESI–MS in the identical way to all other samples (annotation in Fig. S-1 as standards without extraction). Then, the same experiment was repeated, but including the extraction step as for real samples (standards after extraction in Fig. S-1). Relative extraction yields [i.e., ratios of extraction yields of representative standards of selected lipid classes containing C14:0 related to the extraction yield of sphingosyl PE (d17:1/12:0) as the IS] are in the range 90–92 %. The last step was the extraction of selected biological tissues (heart, lung, spleen, and stomach) and also body fluids (plasma and urine) spiked with C14:0 standards followed again by HILIC-HPLC/ESI–MS measurements. Relative extraction yields are between 70 and 96 % (related to standards without extraction) for all standards in Fig. S-1, which is considered as acceptable for such heterogeneous biological materials. The comparison of results obtained by this
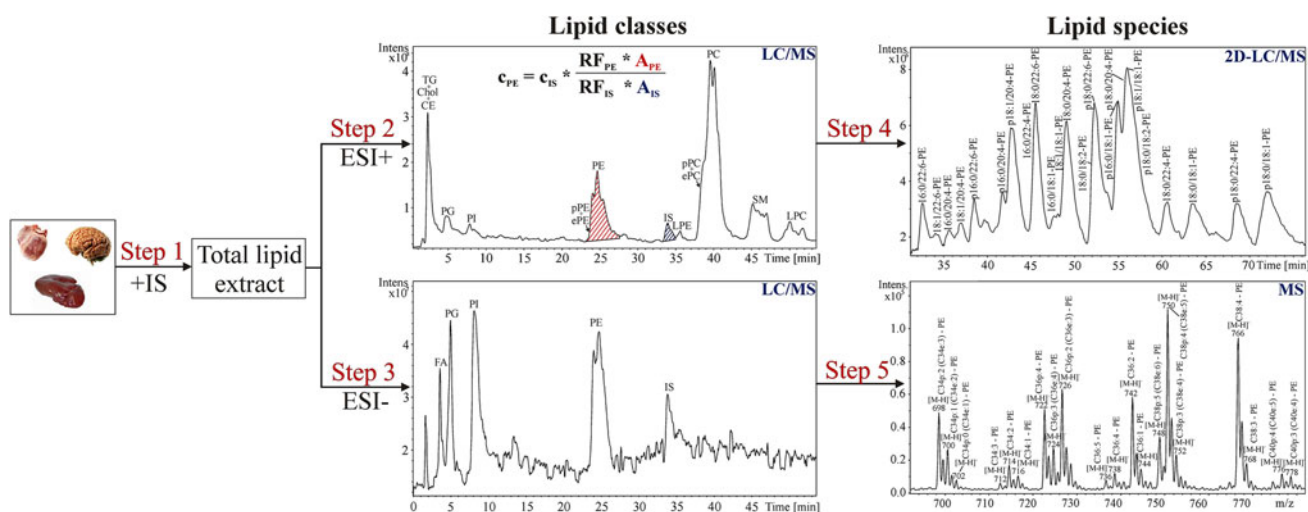
Fig. 1 Schematic overview of our nontargeted lipidomic approach: step 1: extraction with the addition of internal standard; step 2: HILIC-HPLC/MS in the positive-ion ESI; step 3/: HILIC-HPLC/MS in the negative-ion ESI; step 4: off-line 2D-HPLC/MS characterization of individual species inside lipid classes; step 5: negative-ion ESI mass spectrum of separated lipid class in HILIC-HPLC (details in "Materials and Methods")

approach and established quantitation method (SRM on triple quadrupole and ^{31}P NMR) were presented in our previous paper [37].

Lipid Classes Characterization of Porcine Organs Using HILIC-HPLC/ESI–MS

Figure 1 shows an overview of our approach used for the complex lipidomic characterization of eight porcine organs: brain, heart, kidney, liver, lung, spinal cord, spleen, and stomach (all HILIC chromatograms in Figs. S-2 and S-3). This approach is based on our HILIC-HPLC/ESI–MS method published recently [37] for the characterization of three nonpolar lipid classes (triacylglycerols, cholesterol, and cholesteryl esters) and 15 polar lipid classes, from which 10 lipid classes belong to the group of phospholipids such as phosphatidylglycerols (PG), phosphatidylinositols (PI), plasmenylphosphatidylethanolamines (pPE), plasmanylphosphatidylethanolamines (ePE), phosphatidylethanolamines (PE), lysophosphatidylethanolamines (LPE), phosphatidylserines (PS), plasmenylphosphatidylcholines (pPC), plasmanylphosphatidylcholines (ePC), and lysophosphatidylcholines (LPC), and 5 to the group of sphingolipids such as ceramides (Cer), sulfatides, hexosylceramides (HexCer), sphingosylphosphatidylethanolamine (IS), and sphingomyelins (SM). The nontargeted quantitation of lipid classes [37] is based on the peak integration of individual lipid classes separated in the HILIC mode multiplied by their response factors (RF) and correlated by a single IS (sphingosyl PE, d17:1/12:0). However, the HILIC-HPLC method does not enable the separation of non-polar lipids (TG, Chol, and CE), which coelute in one chromatographic

peak close to the void volume of the system, and therefore their quantitation would not be reliable using this chromatographic system. Furthermore, the quantitation of Cer, HexCer, and sulfatides cannot be performed due to wide and only partially resolved peaks occurring in HILIC-HPLC. In the case of PS, the obtained data are semi-quantitative (labeled in Table 1) due to the peak tailing, which causes problems with the peak integration. Reliable quantitative data are obtained for PE, LPE, PC, SM, and LPC [33]. Table 1 shows the comparison of our quantitative data of porcine brain and previously reported data [30, 39, 40] for human or rat brain. Concentrations (in μmol/g) or relative abundances (in %) are similar despite different analytical methods and different types of brain samples (Table 2; Fig. 2). Relative abundances of individual lipid classes in all porcine organs are reported in Fig. 2, where the relative abundance of PC is in the range 32–40 %, PE 26–35 %, SM 5–19 %, PI up to 20 %, PS up to 12 %, LPE up to 8 %, LPC up to 7 %, and PG up to 5 %. Only spleen contains all quantified lipid classes (i.e., PC, PE, PI, SM, PS, LPE, LPC, and PG). In contrast to spleen, the lung and spinal cord are composed from the smallest number of lipid classes (i.e., PC, PE, PI, SM, and PG or PS). The comparison of lipid class concentrations in individual porcine organs (Table 2; Fig. S-4) confirms that PC and PE are the most abundant polar lipids in porcine organs. The highest concentrations of PC and PE are observed in the brain and the lowest in the lung and stomach. The HILIC-HPLC/ESI–MS method enables the determination of total concentrations of lipid classes, but the next step is the determination of concentrations of individual lipid species inside these classes. For this reason, the detailed characterization of

Table 1 Comparison of concentrations (µmol/g) or relative abundances (%) of individual lipid classes in the brain (porcine, human or rat) obtained by our HILIC-HPLC/ESI–MS method and previously published TLC [40], ^{31}P NMR [30], and HPLC/ELSD [39] data

Lipid class	HILIC-HPLC/ESI–MS		TLC [40]	^{31}P NMR [30]		HPLC/ELSD [39]
	Porcine		Human	Human	Rat	Rat
	Concentration (µmol/g)	Relative abundance (%)	Concentration (µmol/g)	Relative abundance (%)		Relative abundance (%)
PI	4.5	5.0	3.7	5.3	3.3	5.3
PE	30.7	34.3	29.0	37.6	37.6	37.6
LPE	2.0	2.3			1.4	
PS	10.6[a]	13.1[a]	9.0	12.5	12.7	15.6
PC	33.2	37.1	22.1	37.6	36.9	37.6
SM	6.5	7.3		1.9	4.8	1.9
LPC	0.8	0.9			1.5	
Others				0.7	0.95	2

[a] Only semi-quantitative data are determined for PS due to the peak tailing

Table 2 Concentrations (µmol/g) of individual lipid classes in porcine organs using the nontargeted quantitation with the single internal standard and response factor approach

Lipid classes	Concentration (µmol/g)							
	Brain	Heart	Kidney	Liver	Lung	Spinal cord	Spleen	Stomach
PG		1.71 ± 0.11	0.88 ± 0.05	0.67 ± 0.01	0.65 ± 0.04		0.27 ± 0.03	0.82 ± 0.01
PI	4.52 ± 0.10	4.99 ± 0.17	12.27 ± 0.63	7.79 ± 0.42	3.58 ± 0.11	5.29 ± 0.12	9.70 ± 0.17	5.02 ± 0.22
PE	30.67 ± 1.04	11.51 ± 0.48	16.22 ± 0.54	14.67 ± 1.26	8.32 ± 0.14	17.49 ± 0.20	16.27 ± 0.59	9.45 ± 0.35
LPE	2.04 ± 0.07[a]	1.60 ± 0.13		3.89 ± 0.17			0.97 ± 0.03[a]	1.48 ± 0.10[a]
PS	10.63 ± 0.83					1.35 ± 0.22	3.03 ± 0.29	
PC	33.21 ± 0.20	13.73 ± 0.87	23.99 ± 0.58	21.06 ± 0.68	11.24 ± 0.19	17.10 ± 0.65	22.51 ± 0.67	11.02 ± 0.22
SM	6.50 ± 0.23	1.87 ± 0.13	7.36 ± 0.29	2.64 ± 0.08	4.12 ± 0.14	9.66 ± 0.22	8.71 ± 0.20	4.38 ± 0.08
LPC	0.84 ± 0.01	1.62 ± 0.02	0.59 ± 0.02	1.78 ± 0.15			0.81 ± 0.04	2.50 ± 0.09

[a] Only semi-quantitation due to the bad peak shapes

selected lipid classes was carried out using two different approaches as described in the next two sections.

Analysis of Individual Lipid Species Using [M−H]$^-$ Ions in Negative-Ion ESI Mass Spectra

This approach enables the characterization of individual lipid species inside lipid classes based on relative abundances of deprotonated molecules [M−H]$^-$ in the negative-ion HILIC-HPLC/ESI–MS (i.e., PE, PI, PG, LPE, HexCer, and sulfatides). This approach cannot be applied for the positive-ion mode due to the presence of both protonated molecules [M+H]$^+$ and sodium adducts [M+Na]$^+$ ions, because [M+Na]$^+$ ions have identical nominal masses as [M+H]$^+$ ions of lipids having more than two methylene units and three double bonds (DB). The resolving power (RP) required for the differentiation of these species is over 300,000 [calculated from m/z 800: RP = $800/(21.98435 - 21.98195) = 333 \times 10^3$]. Such RP

is achievable only on the ion cyclotron resonance mass spectrometer, therefore we have decided on the quantitation of PE, PI, and HexCer species in the negative-ion mode. For PE species, the type of fatty acyl linkage to the glycerol skeleton was also taken into account, i.e., the most commonly known ester-linked fatty acyls at both *sn*-1 and *sn*-2 positions (diacyl) are referred to as PE, ether-linked fatty acyls at the *sn*-1 position (1-alkyl-2-acyl) as ethers (ePE), and vinyl ether-linked fatty acyls at the *sn*-1 (1-alkenyl-2-acyl) as plasmalogens (pPE). Plasmalogens and ethers having identical retention times in the HILIC mode and identical [M−H]$^-$ ions (e.g., plasmalogen C38:4 has the same nominal mass $m/z = 751$ as ether C38:5) cannot be distinguished using this approach. Nevertheless, ether lipids are present in animal tissues as the minority, and therefore they are reported in parentheses (Fig. 3, and the text). The comparison of relative abundances of individual lipid species of PE and pPE (ePE) in all analyzed porcine organs is shown in Fig. 3a and b, respectively.
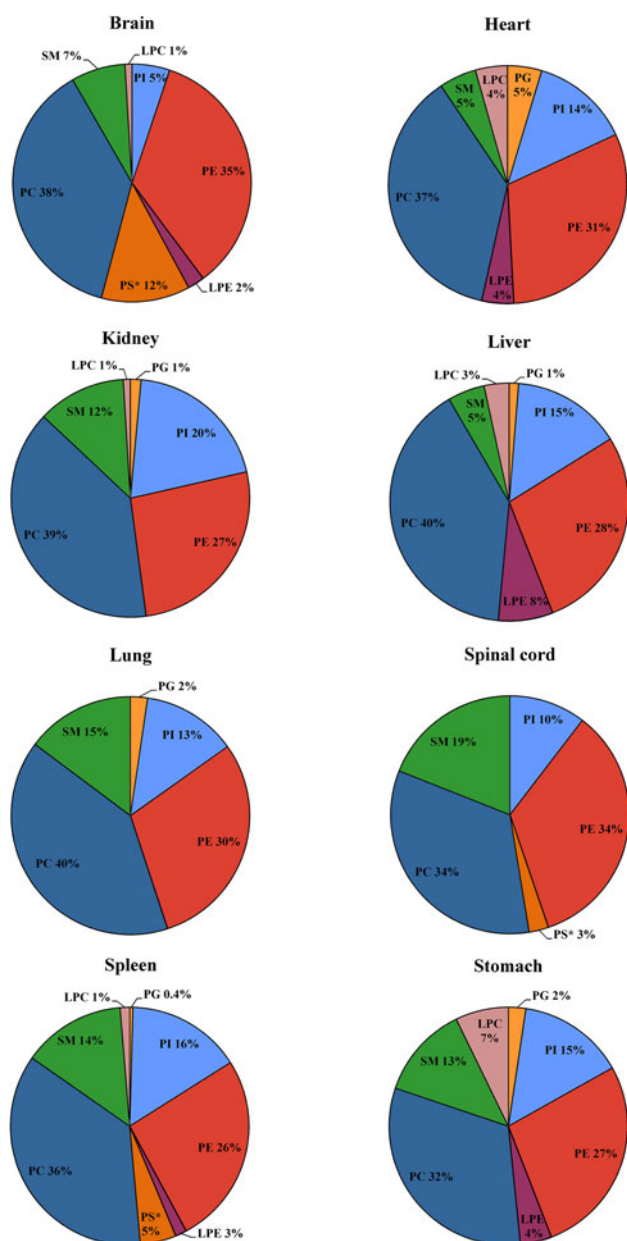
Fig. 2 Relative abundances (%) of monitored lipid classes in porcine organs using the nontargeted quantitation with the single internal standard and response factor approach (color figure online)

Concentrations of individual PE and pPE (ePE) species (Tables S-3, S-4) are calculated from the relative abundances of [M−H]⁻ ions in ESI spectra multiplied by the total concentration of the whole lipid class obtained by nontargeted lipidomic quantitation (Table 2). Fatty acyls are annotated by their CN:DB (carbon number:double bond number). PE (Fig. 3a) containing saturated and monounsaturated fatty acyls with 16 and 18 carbon atoms prevail. The highest relative abundance of PE corresponds to species containing 38 carbon atoms and four DBs (typically C18:0 and C20:4 acyls). Polyunsaturated PE are present

mainly in brain (typical composition C40:6, C40:5, and C40:4) and their lowest relative abundances are observed in heart. Lung, spinal cord, and spleen contain the long-chain (more than 20 carbon atoms) monounsaturated or saturated fatty acyls (C40:1 and C40:2 species), which are typical for sphingolipids, but they also occur in small amounts in phospholipids. There are two cases in which it is not possible to exclude the presence of pPE species in PE (mixtures of C36:0 with C38p:6 and C38:0 with C40p:6) due to identical m/z values observed in ESI spectra. Average parameters of aCN and aDB are calculated in the figure legend. Values of aCN are around 37 carbon atoms, but aDB varies from 2 for spinal cord to 3.3 for heart. Average parameters are useful for the simple overall characterization of particular sample types, as demonstrated earlier for TGs [43].

The representation of pPE (ePE) in various organs shows some interesting features (Fig. 3b). The highest relative abundance of pPE (ePE) is observed in kidney for C36:4 (typically C16:0 and C20:4). The most abundant pPE (ePE) species contains fatty acyls with four and more DBs, which shows that plasmalogens may serve as a source of polyunsaturated fatty acids [4]. Values of aCN in pPE (ePE) species are from 36.7 (heart and kidney) to 38.0 (liver). aDB of individual porcine organs varies from 3.3 (lung) to 4.2 (liver), except for spinal cord (2.8) with higher abundances of pPE (ePE) species containing fatty acyls with 0–3 DBs. In contrast to PE, long-chain saturated and monounsaturated fatty acyls in individual pPE (ePE) occur in spleen and stomach.

In general, plasmalogens can form up to 70 % of PE in animal tissues, where they have many important functions [5, 6]. Therefore, we compare the relative abundance of PE and pPE (ePE) in porcine organs (Fig. 4; Tables S-3, S-4). The lowest amount of pPE (ePE) is found in liver, which could be related to the biosynthesis of fatty acids in liver [5]. On the other hand, nervous tissues (brain and spinal cord) contain the highest amounts of pPE (ePE). The high relative proportion of pPE (ePE) is also observed in porcine heart and stomach. In these organs, plasmalogens have functions of antioxidants, signaling molecules, and modulators of membrane dynamics [5, 6]. Furthermore, individual lipid species of PI (Fig. S-5; Table S-5) were determined, where the highest relative abundance in all porcine organs corresponds to C18:0 and C20:4 fatty acyls (identical as for PE) with the highest abundance in spleen. High proportions of C34:0 and C34:1 PI species are determined in kidney unlike to other organs. Values of aCN are around 37, and aDB are from 2.4 (kidney) to 3.4 (spleen).

This approach was also used for the characterization of relative abundances of individual sphingolipids (i.e., Hex-Cer) containing nonhydroxy-fatty acyls or hydroxy-fatty
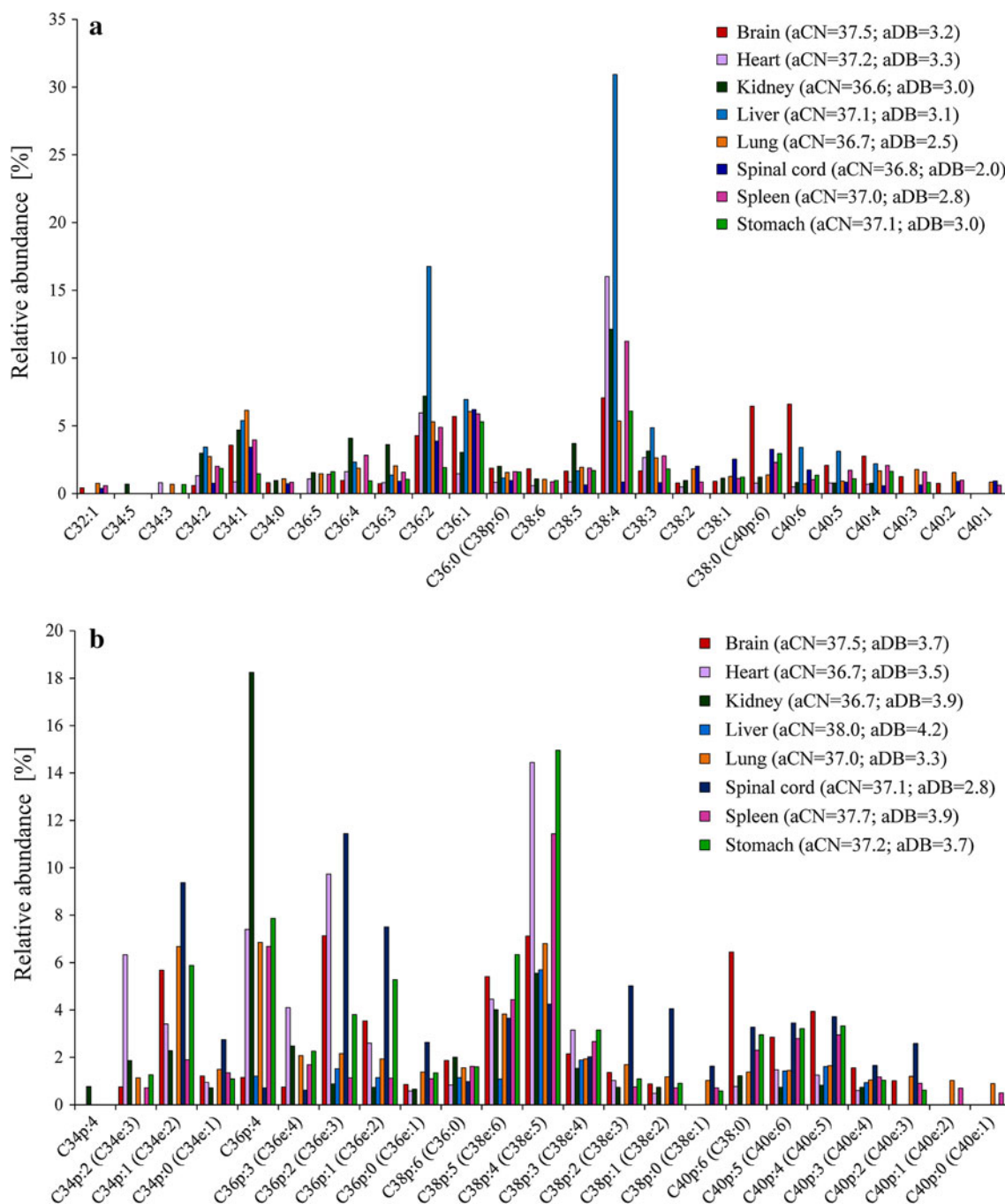
Fig. 3 Relative abundances (%) of individual species of (**a**) PE (1,2–diacyl) and (**b**) pPE (1-alkenyl-2-acyl) and ePE (1-alkyl-2-acyl) determined using relative abundances of [M−H]⁻ ions in the negative-ion HILIC-HPLC/ESI–MS and calculated average carbon numbers (aCN) and average double bonds (aDB) numbers in porcine organs

acyls in porcine brain, kidney, spleen, spinal cord, and stomach (Fig. 5). HexCer are the most abundant in nervous tissues (brain and spinal cord), where they form important components of neurons [2]. Moreover, they are heavily represented in spleen due to various functions in the immune system [2]. Each organ has different HexCer with the highest relative abundance, i.e., C42:1-OH (C43:0) and C42:2-OH (C43:2) in brain and spinal cord, and C36:2-OH

(C37:1) and C36:0-OH in stomach. Kidney and spleen contain the most abundant nonhydroxy-fatty acyls, such as C40:1 (C39:2-OH) and C40:0 (C39:1-OH) in kidney and C41:2 (C40:3-OH) and C39:2 (C38:3-OH) in spleen. As for plasmalogens and ethers, lipid species having identical values of [M−H]⁻ ions for fatty acyls containing non-hydroxy- and hydroxy-forms (e.g., HexCer containing C42:2-OH has the same nominal value of $m/z = 825$ as

Fig. 4 Comparison of total concentrations of PE (individual species shown in Fig. 3a) and the sum of pPE and ePE species (individual species shown in Fig. 3b) in porcine organs
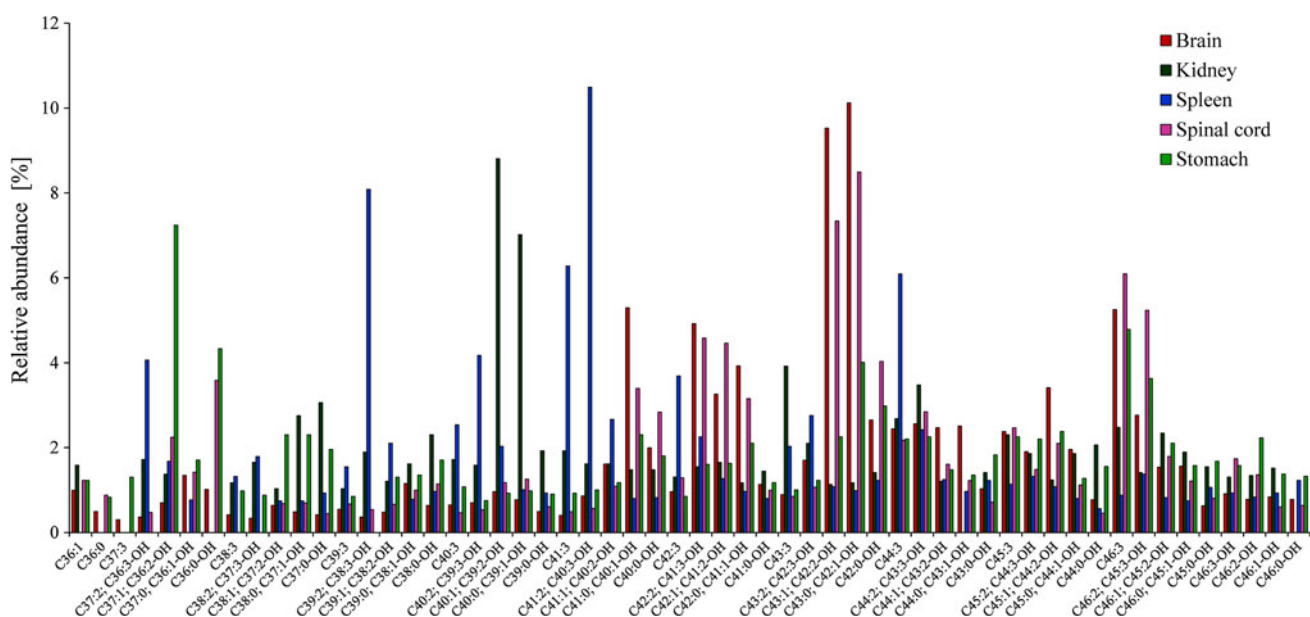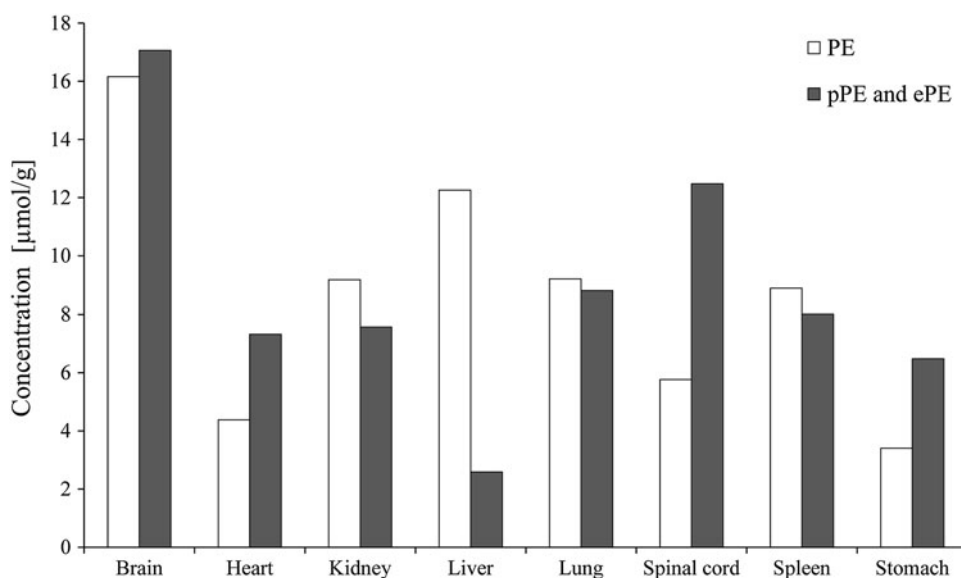

Fig. 5 Relative abundances (%) of individual HexCer containing nonhydroxy- or hydroxy-fatty acyls in brain, kidney, spleen, spinal cord, and stomach determined using relative abundances of [M−H]⁻ ions in the negative-ion HILIC-HPLC/ESI–MS

HexCer containing C43:2) cannot be distinguished using this approach. Fatty acyls in parentheses are less probable due to the odd carbon number or higher number of DBs, because saturated and monounsaturated fatty acyls are typical for glycosphingolipids.

Off-Line 2D-HPLC/MS Detailed Analysis of Individual Lipid Species in Porcine Brain

The limitation of the first approach is that the only information on the total number of carbon atoms and DBs is obtained without the knowledge of the attached fatty acyls

and their positions on the glycerol skeleton. For this reason, off-line two-dimensional HILIC × RP-HPLC/ESI–MS has been used for the detailed analysis of porcine brain. Individual fractions of lipid classes separated by HILIC-HPLC are isolated and used in the second dimension for the separation of individual lipid species inside lipid classes according to the fatty acyl chain lengths and the number of DBs using RP-HPLC. Almost 70 phospholipid (Table S-6) and 100 sphingolipid species are identified in the porcine brain. Namely, 11 PI (Fig. S-6A), 12 PE and 10 pPE published in [18], 7 LPE and 3 pLPE, 17 species of PC, 2 pPC and 2 ePC (Fig. 6a), and 5 LPC, and 42 are HexCer

and 2 Cer (Fig. 6b), 38 sulfatides (Fig. S-6B), and 12 SM. Phospholipids (PC, PE, and PI) are formed by the combination of 14 fatty acyls containing 16–22 carbon atoms and 0–6 DBs, where the most abundant fatty acyls are C16:0, C18:0, C18:1, and C20:4, whereas sphingolipids (HexCer, Cer, sulfatides, and SM) consist of 15 fatty acyls (nonhydroxy and hydroxy) containing 16–26 carbon atoms and 0–2 DBs. Fatty acyl positions on the glycerol skeleton are determined according to relative abundances of fatty acyls fragment ions [RCOO]$^-$ in the negative-ion ESI spectra. Higher relative abundances of [RCOO]$^-$ ions are typically related to the fragmentation from the sn-2 position compared to the sn-1 position for studied phospholipids (Fig. 7), but relative abundances of these fragment ions are also strongly affected by their unsaturation degree. Exceptions are observed in the case of some phospholipids containing combinations of C18:0 and C22:6, in which ratios of [RCOO]$^-$ ions are affected by the presence of [RCOO]$^-$ ion of polyunsaturated FA [44]. The second

diagnostic ions for the determination of sn-2 are the neutral losses of ketene [M-H-RCHCO]$^-$ (Fig. 7) or fatty acid [M-H-RCOOH]$^-$. Neutral losses from the sn-2 position resulting in the formation of [M-H-RCHCO]$^-$ ions are always preferred without exception for PC, pPC, ePC, PE, pPE, ePE, PI, HexCer, and sulfatides studied in this work. It has been reported in the literature that the reversed ratio of above mentioned fragment ions has been observed for some lipid classes, such as PS and PA [44].

We observed a strong preference of polyunsaturated fatty acyls in the sn-2 position (Fig. 7a). The preference of sn-positions for two saturated fatty acyls (18:0/16:0-PC) is related to the acyl chain length, because fatty acyls containing more carbon atoms (C18:0) are favored in the sn-1 position unlike fatty acyls containing fewer carbon atoms (C16:0) in thes sn-2 position (Fig. 7b). HexCer (Fig. 6b) and sulfatides (Fig. S-6B) are separated in RP-HPLC according to nonhydroxy- or hydroxy-form of their fatty acyls, lengths, and the number of DBs. Nonhydroxy-forms

Fig. 6 Off-line 2D-HPLC/ESI–MS analysis of (a) PC and (b) HexCer and Cer fractions from the porcine brain. RP-HPLC conditions: flow rate 0.3 mL/min, separation temperature 40 °C, gradient 0 min—75 % A + 25 % B, 110 min—89 % A + 11 % B, where A is the mixture of acetonitrile–2-propanol (1:1, v/v) and B is 5 mM aqueous ammonium acetate
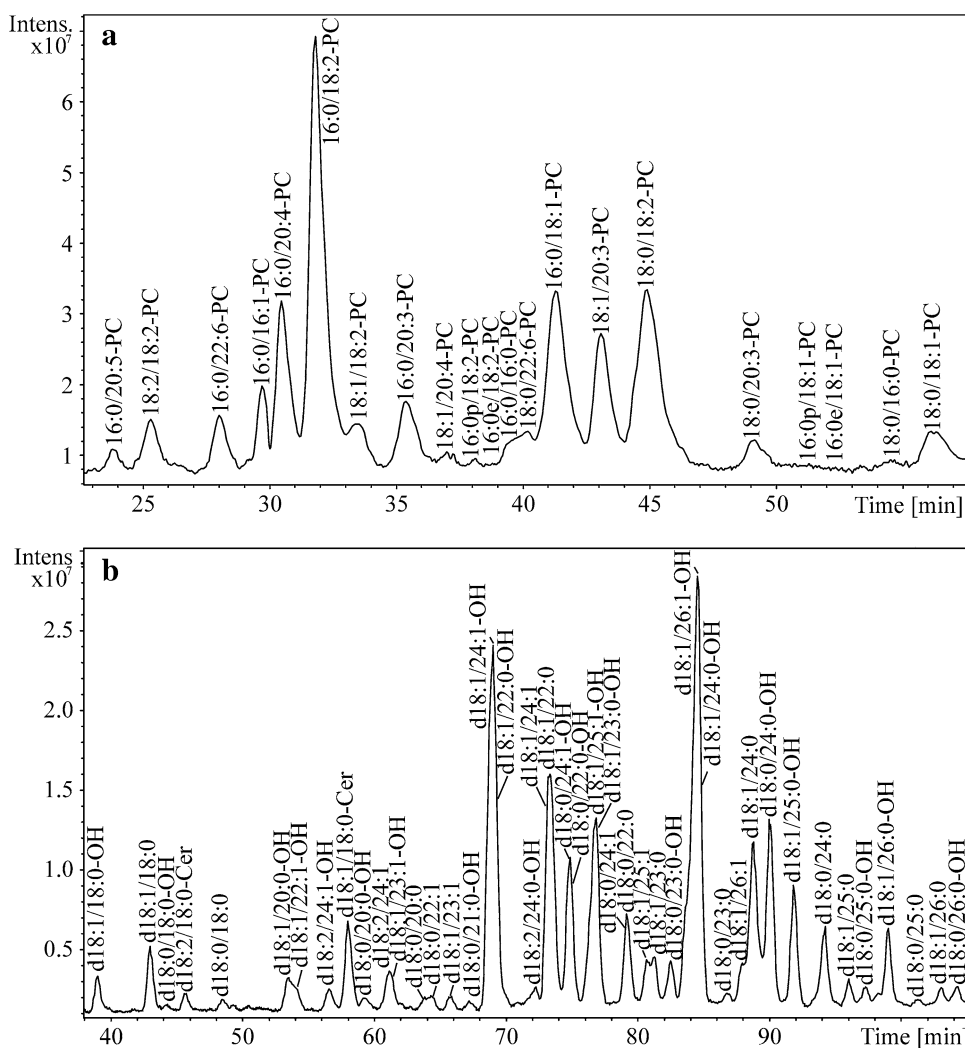
Fig. 7 Negative-ion ESI–MS/MS spectra of (a) *m/z* 766 for [M−H]⁻ ion of 1-stearoyl-2-arachidonoyl-*sn*-glycero-3-phosphoethanolamine (16:0/20:4-PE), and (b) *m/z* 746 for [M-CH₃]⁻ ion of 1-stearoyl-2-palmitoyl-*sn*-glycero-3-phosphocholine (18:0/16:0-PC)
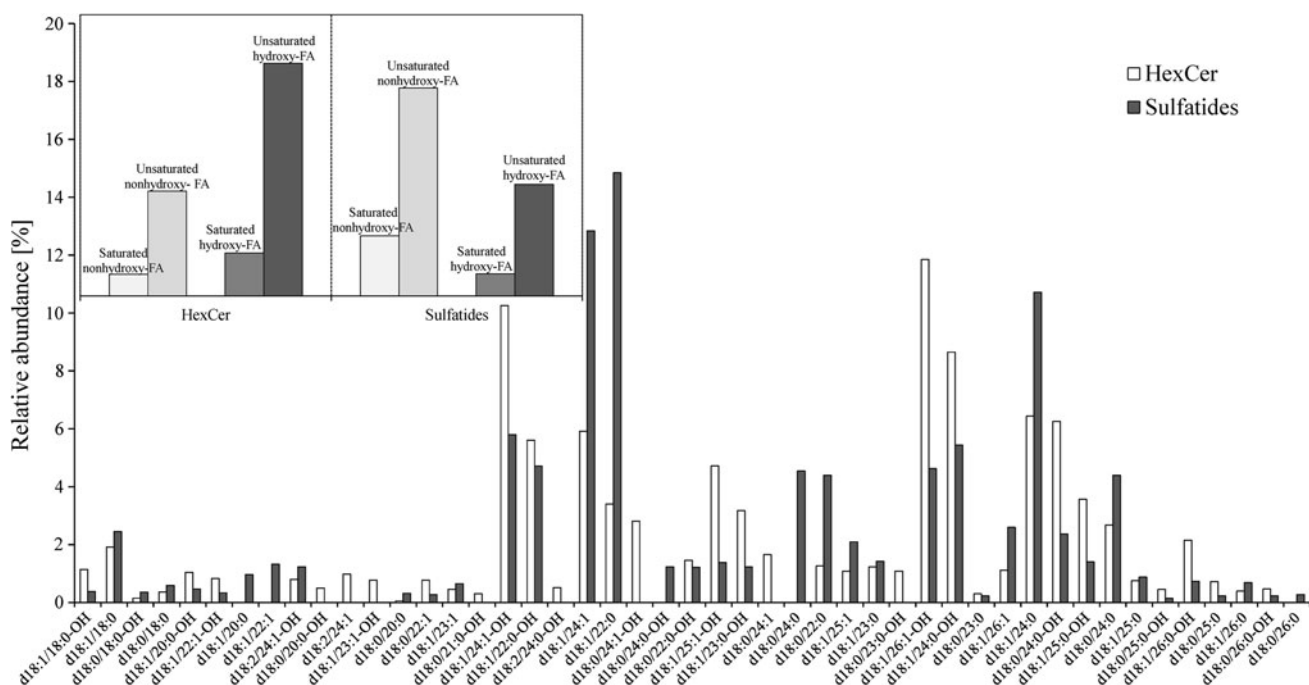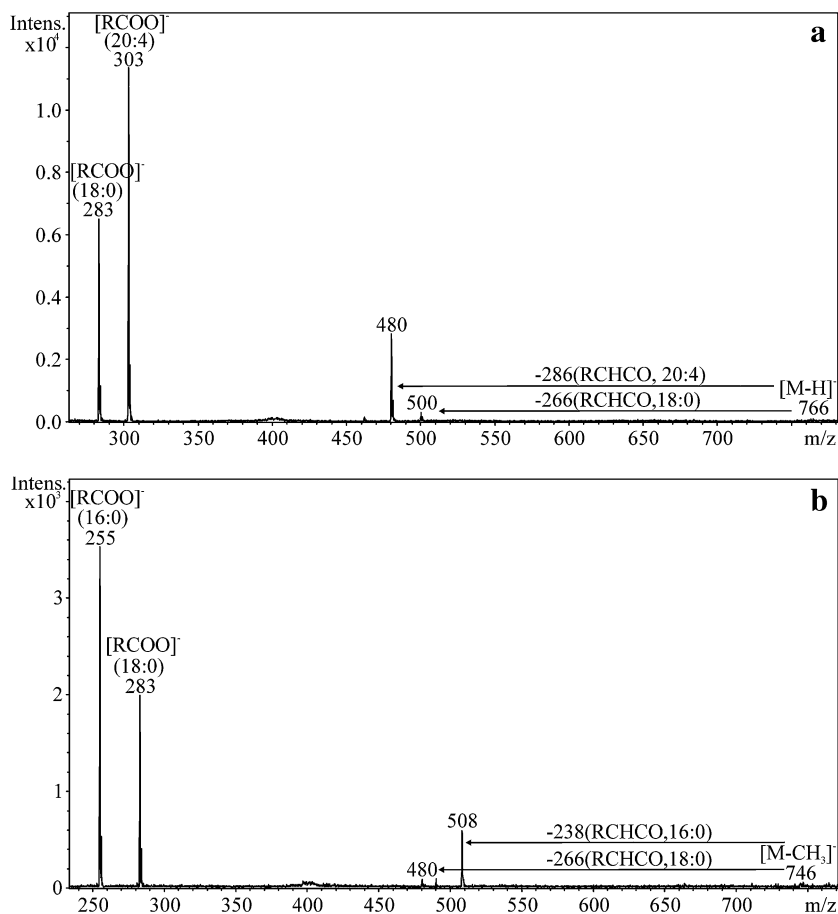

Fig. 8 Comparison of relative abundances of fatty acyl combinations in hexosylceramides (HexCer) and sulfatides in the porcine brain, and the distribution of saturated and unsaturated nonhydroxy- and hydroxy-fatty acyls in HexCer and sulfatides (inset)

Table 3 Relative molar concentrations (%) of fatty acids identified in porcine organs using GC/FID, retention times (t_R) of their FAMEs, response factors (RF), average carbon number (aCN) and average double bond (aDB) numbers

t_R [min]	Fatty acid	RF	Brain	Heart	Kidney	Liver	Lung	Spinal cord	Spleen	Stomach
8.7	C14:0	1.03	0.5	1.3	0.4		1.5	0.4	0.5	1.1
9.9	C15:0	1.04	0.1		0.2		0.3	0.1	0.5	0.3
11.4	C16:0	1.00	24.2	27.0	23.6	13.6	27.4	16.1	31.6	24.8
12.3	Δ9-C16:1	1.04	0.8	1.3	0.3	1.5	2.1	0.7	0.5	1.5
13.2	C17:0	0.99	0.3	0.5	1.0	0.3	0.6	0.4	1.2	1.5
15.2	C18:0	0.98	21.0	18.5	16.9	31.3	12.8	16.8	17.5	17.0
16.1	Δ9-C18:1	0.99	21.1	25.7	13.7	16.1	39.9	39.2	11.1	41.1
16.3	Δ11-C18:1	1.01	5.6	3.0	3.4	1.4	3.5	7.7	2.6	3.0
17.6	Δ9,12-C18:2	1.00	0.4	13.8	12.8	13.2	4.5	0.5	5.6	3.7
19.5	Δ9,12,15-C18:3	0.99		0.3	0.2		0.1		0.1	0.2
19.6	C20:0	0.98	0.1	0.2	0.2			0.6	0.1	0.2
20.6	Δ11-C20:1	0.99	0.7	0.5	0.4		0.9	6.2	0.4	1.0
21.8	C20:2	1.00[a]	0.3					0.5		
22.3	Δ11,14-C20:2	0.99	0.1	0.3	0.6		0.4	0.2	0.5	0.3
22.6	C20:3	1.00[a]	0.7		0.2	0.7		0.3	0.2	0.1
23.5	Δ8,11,14-C20:3	0.99	0.4	0.3	1.8	0.8	0.3	0.5	1.1	0.2
24.2	Δ5,8,11,14-C20:4	0.97	8.6	4.8	19.7	13.0	3.3	3.5	19.2	2.4
25.5	Δ13-C22:1	0.97	0.2		0.1			1.2	0.1	
26.2	Δ5,8,11,14,17-C20:5	1.00	0.2	0.3	1.5	1.7	0.2	0.1	0.5	0.1
26.3	C23:0	0.96	0.2					0.2		
26.9	C24:0[b]	1.00[a]	0.6					0.4	0.1	
28.0	Δ7,10,13,16-C22:4	0.97	3.5	0.6	0.6	1.0	0.9	2.1	2.8	0.6
28.5	Δ4,7,10,13,16-C22:5	0.96	1.0		0.1			0.1	0.2	
29.5	Δ7,10,13,16,19-C22:5	0.98	0.4	0.3	0.6	1.4	0.3	0.2	2.3	0.3
29.9	Δ4,7,10,13,16,19-C22:6	1.03	8.6		1.3	0.9	0.2	1.9	1.3	0.2
31.4	C26:0[b]	1.00[a]	0.2					0.1		
32.0	C27:0[b]	1.00[a]	0.3	1.3	0.4	3.0	1.0	0.2		0.3
aCN			18.5	17.8	18.2	18.6	17.7	18.3	18.2	17.6
aDB			1.5	0.9	1.6	1.3	0.8	1.0	1.5	0.7

[a] Not measured due to the lack of standard

[b] Branched fatty acids

of fatty acyls have higher retention times then their hydroxy-forms, as illustrated in examples for HexCer (Δt_R = 4–4.5 min) and sulfatides (2.5–3 min). The comparison of relative abundance of individual lipid species in HexCer and sulfatides is shown in Fig. 8. Major sphingolipids are composed of ceramide possessing 4-sphingenine (d18:1; prefix "d" designates a dihydroxy sphingoid base) with the hydroxy-form of C26:1, C24:1, and C24:0 acyls for HexCer and the nonhydroxy-form of C22:0, C24:1, and C24:0 acyls for sulfatides. The representation of nonhydroxy- and hydroxy-forms of fatty acyls in HexCer is in the ratio 30/70, which is exactly the opposite for sulfatides with the ratio 70/30 (Fig. 8 inset). HexCer are composed of 22 % saturated and 78 % unsaturated fatty acyls, while sulfatides have 43 % saturated and 57 % unsaturated fatty acyls.

Fatty Acid Profiling Using GC/FID

The fatty acid composition of porcine organs is characterized by the GC/FID analysis of FAMEs after the transesterification of total lipid extracts with sodium methoxide (Table 3). The previously optimized GC/FID method [9] enables the separation of FAMEs according to the acyl chain length and the number of DBs (Fig. S-7). Fatty acid profiles of analyzed porcine organs are obtained from peak areas of FAMEs in GC/FID chromatograms multiplied by the RFs of identical standards related to C16:0, and a total of 23 different fatty acids containing 14–26 carbon atoms and 0–6 DBs were determined. The most abundant fatty acid is C16:0 in brain, kidney, and spleen, Δ9-C18:1 in heart, lung, spinal cord, and stomach,

and C18:0 in liver. Large differences in the relative abundance of fatty acids are observed for arachidonic acid (C20:4), which is a key inflammatory intermediate [4]. Arachidonic acid forms approximately 20 % of identified fatty acids in porcine kidney and spleen, 14 % in liver, 9 % in brain, and 5 % or less in heart, lung, spinal cord, and stomach. The highest proportion of polyunsaturated fatty acids is determined in brain, while the lowest abundance is observed in heart. Average parameters are also calculated for fatty acid profiles of analyzed organs similar to the HPLC/MS determination of aCN and aDB in individual lipid classes. Values of aCN are around 18, but aDB varies from 0.7 for stomach to 1.6 for kidney.

Conclusions

The nontargeted HILIC-HPLC/ESI–MS method enables the characterization of individual lipid classes and their representation in vital porcine organs, such as brain, heart, kidney, liver, lung, spinal cord, spleen, and stomach. Concentrations of individual lipid classes in porcine organs were compared with previously published data. The determination of individual lipid species inside these classes was performed based on relative abundances of deprotonated molecules $[M-H]^-$ in the negative-ion ESI mode and off-line 2D-HPLC/MS. The first approach using $[M-H]^-$ ions provides important information on PE and their plasmalogens or ether analogs, PI, and HexCer in studied organs. Off-line 2D-HPLC/MS has been applied for the detailed analysis of porcine brain including the determination of attached fatty acyls and their positions on the glycerol ividual organs was performed using average parameters of CN and DB. The complementary information on fatty acid profiles was obtained by GC/FID. The comprehensive lipidomic analysis provides the detailed knowledge of the lipidome, which will be applied for future metabolic studies on human to investigate serious lipid-related human disorders.

References

1. Fahy E, Subramaniam S, Brown HA, Glass CK, Merrill AH, Murphy RC, Raetz CRH, Russell DW, Seyama Y, Shaw W, Shimizu T, Spener F, van Meer G, VanNieuwenhze MS, White SH, Witztum JL, Dennis EA (2005) A comprehensive classification system for lipids. J Lipid Res 46:839–861
2. Christie WW (2012) The lipid library. http://lipidlibrary.aocs.org/
3. Brown HA, Murphy RC (2009) Working towards an exegesis for lipids in biology. Nat Chem Biol 5:602–606
4. Calder PC (2006) n-3 polyunsaturated fatty acids, inflammation, and inflammatory diseases. Am J Clin Nutr 83:1505S–1519S
5. Braverman NE, Moser AB (2012) Functions of plasmalogen lipids in health and disease. Biochim Biophys Acta 1822:1442–1452
6. Nagan N, Zoeller RA (2001) Plasmalogens: biosynthesis and functions. Prog Lipid Res 40:199–229
7. Santos CR, Schulze A (2012) Lipid metabolism in cancer. FEBS J 279:2610–2623
8. Hamilton S, Hamilton RJ, Sewell PA (1992) Lipid analysis: practical approach. Oxford University Press, New York
9. Lísa M, Netušilová K, Franěk L, Dvořáková H, Vrkoslav V, Holčapek M (2011) Characterization of fatty acid and triacylglycerol composition in animal fats using silver-ion and non-aqueous reversed-phase high-performance liquid chromatography/mass spectrometry and gas chromatography/flame ionization detection. J Chromatogr A 1218:7499–7510
10. Cvačka J, Hovorka O, Jiroš P, Kindl J, Stránský K, Valterová I (2006) Analysis of triacylglycerols in fat body of bumblebees by chromatographic methods. J Chromatogr A 1101:226–237
11. Holčapek M, Lísa M, Jandera P, Kabátová N (2005) Quantitation of triacylglycerols in plant oils using HPLC with APCI-MS, evaporative light-scattering, and UV detection. J Sep Sci 28:1315–1333
12. Lísa M, Holčapek M (2008) Triacylglycerols profiling in plant oils important in food industry, dietetics and cosmetics using high-performance liquid chromatography-atmospheric pressure chemical ionization mass spectrometry. J Chromatogr A 1198:115–130
13. Ahn EJ, Kim H, Chung BC, Kong G, Moon MH (2008) Quantitative profiling of phosphatidylcholine and phosphatidyletha-nolamine in a steatosis/fibrosis model of rat liver by nanoflow liquid chromatography/tandem mass spectrometry. J Chromatogr A 1194:96–102
14. Axelsen PH, Murphy RC (2010) Quantitative analysis of phospholipids containing arachidonate and docosahexenoate chains in microdissected regions of mouse brain. J Lipid Res 51:660–671
15. Bang DY, Ahn EJ, Moon MH (2007) Shotgun analysis of phospholipids from mouse liver and brain by nanoflow liquid chromatography/tandem mass spectrometry. J Chromatogr B 852:268–277
16. Retra K, Bleijerveld OB, van Gesteil RA, Tielens AGM, van Hellemond JJ, Brouwers JF (2008) A simple and universal method for the separation and identification of phospholipid molecular species. Rapid Commun Mass Spectrom 22:1853–1862
17. Taguchi R, Ishikawa M (2010) Precise and global identification of phospholipid molecular species by an orbitrap mass spectrometer and automated search engine lipid search. J Chromatogr A 1217:4229–4239
18. Lísa M, Cífková E, Holčapek M (2011) Lipidomic profiling of biological tissues using off-line two-dimensional high-performance liquid chromatography mass spectrometry. J Chromatogr A 1218:5146–5156
19. Cvačka J, Svatoš A (2003) Matrix-assisted laser desorption/ionization analysis of lipids and high molecular weight hydrocarbons with lithium 2,5-dihydroxybenzoate matrix. Rapid Commun Mass Spectrom 17:2203–2207
20. Fuchs B, Schiller J (2009) Application of MALDI-TOF mass spectrometry in lipidomics. Eur J Lipid Sci Technol 111:83–98
21. Jackson SN, Wang HYJ, Woods AS (2005) In situ structural characterization of phosphatidylcholines in brain tissue using MALDI-MS/MS. J Am Soc Mass Spectrom 16:2052–2056
22. Dugo P, Kumm T, Crupi ML, Cotroneo A, Mondello L (2006) Comprehensive two-dimensional liquid chromatography

combined with mass spectrometric detection in the analyses of triacylglycerols in natural lipidic matrixes. J Chromatogr A 1112:269–275

23. Sandra K, Pereira AD, Vanhoenacker G, David F, Sandra P (2010) Comprehensive blood plasma lipidomics by liquid chromatography/quadrupole time-of-flight mass spectrometry. J Chromatogr A 1217:4087–4099

24. Byrdwell WC (2010) Dual parallel mass spectrometry for lipid and vitamin D analysis. J Chromatogr A 1217:3992–4003

25. Han XL, Yang K, Gross RW (2012) Multi-dimensional mass spectrometry-based shotgun lipidomics and novel strategies for lipidomic analyses. Mass Spectrom Rev 31:134–178

26. Yang K, Han X (2011) Accurate quantification of lipid species by electrospray ionization mass spectrometry—meets a key challenge in lipidomics. Metabolites 1:21–40

27. Yang K, Cheng H, Gross RW, Han XL (2009) Automated lipid identification and quantification by multidimensional mass spectrometry-based shotgun lipidomics. Anal Chem 81:4356–4368

28. Hu CX, van der Heijden R, Wang M, van der Greef J, Hankemeier T, Xua GW (2009) Analytical strategies in lipidomics and applications in disease biomarker discovery. J Chromatogr B 877:2836–2846

29. Culeddu N, Bosco M, Toffanin R, Pollesello P (1998) P-31 NMR analysis of phospholipids in crude extracts from different sources: improved efficiency of the solvent system. Magn Reson Chem 36:907–912

30. Pearce JM, Komoroski RA (2000) Analysis of phospholipid molecular species in brain by P-31 NMR spectroscopy. Magn Reson Med 44:215–223

31. Berdeaux O, Juaneda P, Martine L, Cabaret S, Bretillon L, Acar N (2010) Identification and quantification of phosphatidylcholines containing very-long-chain polyunsaturated fatty acid in bovine and human retina using liquid chromatography/tandem mass spectrometry. J Chromatogr A 1217:7738–7748

32. Hsu FF, Turk J (2001) Studies on phosphatidylglycerol with triple quadrupole tandem mass spectrometry with electrospray ionization: fragmentation processes and structural characterization. J Am Soc Mass Spectrom 12:1036–1043

33. Quehenberger O, Armando AM, Brown AH, Milne SB, Myers DS, Merrill AH, Bandyopadhyay S, Jones KN, Kelly S, Shaner RL, Sullards CM, Wang E, Murphy RC, Barkley RM, Leiker TJ, Raetz CRH, Guan ZQ, Laird GM, Six DA, Russell DW, McDonald JG, Subramaniam S, Fahy E, Dennis EA (2010) Lipidomics reveals a remarkable diversity of lipids in human plasma. J Lipid Res 51:3299–3305

34. Shaner RL, Allegood JC, Park H, Wang E, Kelly S, Haynes CA, Sullards MC, Merrill AH (2009) Quantitative analysis of sphingolipids for lipidomics using triple quadrupole and quadrupole linear ion trap mass spectrometers. J Lipid Res 50:1692–1707

35. Sommer U, Herscovitz H, Welty FK, Costello CE (2006) LC-MS-based method for the qualitative and quantitative analysis of complex lipid mixtures. J Lipid Res 47:804–814

36. Stahlman M, Ejsing CS, Tarasov K, Perman J, Boren J, Ekroos K (2009) High-throughput shotgun lipidomics by quadrupole time-of-flight mass spectrometry. J Chromatogr B 877:2664–2672

37. Cífková E, Holčapek M, Lísa M, Ovčačíková M, Lyčka A, Lynen F, Sandra P (2012) Nontargeted quantitation of lipid classes using hydrophilic interaction liquid chromatography–electrospray ionization mass spectrometry with single internal standard and response factor approach. Anal Chem 84:10064–10070

38. Dreissig I, Machill S, Salzer R, Krafft C (2009) Quantification of brain lipids by FTIR spectroscopy and partial least squares regression. Spectrochim Acta A 71:2069–2075

39. Homan R, Anderson MK (1998) Rapid separation and quantitation of combined neutral and polar lipid classes by high-performance liquid chromatography and evaporative light-scattering mass detection. J Chromatogr B 708:21–26

40. Igarashi M, Ma KZ, Gao F, Kim HW, Greenstein D, Rapoport SI, Rao JS (2010) Brain lipid concentrations in bipolar disorder. J Psychiatr Res 44:177–182

41. Kakela R, Somerharju P, Tyynela J (2003) Analysis of phospholipid molecular species in brains from patients with infantile and juvenile neuronal-ceroid lipofuscinosis using liquid chromatography-electrospray ionization mass spectrometry. J Neurochem 84:1051–1065

42. Folch J, Lees M, Stanley GHS (1957) A simple method for the isolation and purification of total lipides from animal tissues. J Biol Chem 226:497–509

43. Lísa M, Holčapek M, Boháč M (2009) Statistical evaluation of triacylglycerol composition in plant oils based on high-performance liquid chromatography-atmospheric pressure chemical ionization mass spectrometry data. J Agric Food Chem 57:6888–6898

44. Hsu FF, Turk J (2009) Electrospray ionization with low-energy collisionally activated dissociation tandem mass spectrometry of glycerophospholipids: mechanisms of fragmentation and structural characterization. J Chromatogr B 877:2673–2695